

1 **Discriminating underground nuclear explosions leading**  
2 **to late-time radionuclide gas seeps**

3 **Dylan R. Harp, S. Michelle Bourret, Philip H. Stauffer, and Edward M.**  
4 **Kwicklis**

5 Computational Earth Science, Los Alamos National Laboratory, Los Alamos, NM, 87545

6 **Key Points:**

- 7 • Barometric-pumping efficiency facilitates discrimination of underground nuclear  
8 explosions leading to late-time seeps.  
9 • Longer high-efficiency barometric periods and higher high-efficiency amplitudes  
10 indicate a greater chance of late-time seeps.  
11 • Low air-filled porosity indicates a greater chance of late-time seeps.

**Abstract**

Utilizing historical data from the U.S. nuclear test program and freely available barometric pressure data, we performed an analytical barometric-pumping efficiency analysis to determine factors resulting in late-time radionuclide gas seeps from underground nuclear explosions. We considered sixteen underground nuclear explosions with similar geology and test setup, of which five resulted in the measurement of late-time radionuclide gas concentrations at the ground surface. The factors we considered include barometric frequency and amplitude, depth of burial, air-filled porosity, intact-rock permeability, fracture aperture, and fracture spacing. The analysis indicates that the best discriminators of late-time radionuclide gas seeps for these explosions are barometric frequency and amplitude and air-filled porosity. While geologic information on fracture aperture and spacing is not available for these explosions, the sensitivity of barometric-pumping efficiency to fracture aperture indicates that fracture aperture would likely also be a good discriminator.

**Plain Language Summary**

Variations in air pressures (barometric variations) can drive gases created during underground nuclear explosions to the ground surface. The changes in air pressure above the ground push and pull the air in connected spaces between rocks (fractures) allowing these pressure changes to access 100s of meters into the subsurface. Some barometric variations and geologies are more conducive to driving gases to the ground surface than others. Using a model that combines the effect of the barometric variations and geology, we are able to identify scenarios that are more likely to lead to gases arriving at the ground surface after an underground nuclear explosion. Identifying underground nuclear explosions that will likely result in gases arriving at the ground surface and entering the atmosphere provides information for investigators trying to verify nuclear test ban treaties.

**1 Introduction**

Verifying adherence of signatory countries to nuclear test ban treaties, such as the Comprehensive Nuclear Test Ban Treaty (CTBT), requires the ability to detect clandestine nuclear tests. In order to take advantage of the containment and obscurity provided by the subsurface, clandestine nuclear tests will likely be in the form of an underground nuclear explosion (UNE). Detecting radionuclide gases seeping at the ground surface of a suspected UNE site will provide “smoking gun” evidence of a clandestine UNE (Kalinowski et al., 2010; Sun & Carrigan, 2014). Identifying the factors that will increase the chance of late-time seeps after a clandestine UNE will help determine if radionuclide gases should be expected to be detected at the ground surface near the UNE site or in the atmosphere.

While prompt releases of radionuclide gas due to a severe containment failure could occur within minutes to a few hours after a UNE, late-time releases at the ground surface to the atmosphere due to barometrically driven gas transport (referred to as late-time seeps (United States Congress, 1989)) could occur from days to months afterwards. The occurrence of a late-time seep will depend on the complex process of barometrically driven subsurface gas transport, commonly referred to as *barometric pumping*, whereby increasing barometric pressure drives atmospheric air into the subsurface through fractures and decreasing barometric pressure draws subsurface air towards the ground surface (Nilson et al., 1991; Auer et al., 1996; Neeper, 2003; Neeper & Stauffer, 2012). Storage in the intact rock pore space (air and water filled) result in a ratcheting of gases towards the surface in between barometric cycles resulting in significantly faster transport than would occur due to diffusive transport alone (Nilson et al., 1991; Harp et al., 2019). The process of barometric pumping involves advective flow through fractures, diffusive transport in intact rock, dissolution/exolution from pore-water (Harp et al., 2018), iso-

topic fractionation, and transport due to explosion-induced pressure and temperature gradients (Sun & Carrigan, 2016). Factors controlling the rate of gas transport can include subsurface properties, such as air-filled porosity, saturation, fracture aperture (i.e., permeability), and intact rock diffusivity (Jordan et al., 2014), and the characteristics of the barometric pressure signal before and after the UNE, such as amplitude and frequency (Harp et al., 2019). Factors associated with UNE design will also affect the likelihood of late-time seeps, such as depth of burial, yield, fissile material, etc.

In this study, we analyze the importance of barometric frequency and amplitude, air-filled porosity, rock-matrix permeability, and depth of burial as discriminating factors in determining the potential for late-time seeps from UNEs. We evaluate these factors using an analytical barometric-pumping efficiency analysis approach presented in Harp et al. (2019) and briefly summarized in Section 2. We performed the analysis on barometric and site data associated with 16 historic U.S. UNEs collected and evaluated in Bourret, Kwicklis, Harp, et al. (2019) and briefly described in Section 3. In Section 4, we present a thorough analysis of the factors, including a comparison of barometric-pumping efficiencies between UNEs with and without late-time seeps and an analysis of the sensitivity of the barometric-pumping efficiency to the factors. In Section 5, we discuss the implications of the results for discriminating late-time seeps from UNEs. In Section 6, we provide a list of conclusions from the research.

## 2 Methods

We use an analytical approach to quantify barometric-pumping efficiency based on analytical solutions derived by Nilson et al. (1991) described in detail in Harp et al. (2019). The analytical approach is briefly described here.

Barometric-pumping efficiency quantifies the ability of a barometric component (i.e., a single frequency/amplitude pair, where a barometric signal is composed of many barometric components) to extract gas from the subsurface to the atmosphere. It is comprised of three factors: (1) the ability of the barometric component to push a packet of atmospheric air to the depth of the gas in the subsurface and extract the packet of air back to the atmosphere; (2) if the timing of the barometric component is such that gas-contaminated air has time to exchange with the atmospheric packet of air; and (3) how often the barometric component occurs (i.e., its frequency).

The first factor is captured in the *breathing efficiency*  $\eta_B$ , which quantifies the volume of air that a barometric cycle is able to extract relative to the maximum volume that could be removed if the subsurface were in perfect equilibrium with the atmosphere (i.e., if the subsurface had infinite pneumatic diffusivity). The second factor is captured in the *diffusive exchange efficiency*  $\eta_D$ , which quantifies the fraction of the mass of tracer that is removed versus the maximum that would be removed if the concentration of the packet of air could achieve and maintain the concentration of gas at depth during its return to the ground surface. The third factor is the barometric component frequency,  $\omega$ , which accounts for the fact that given two barometric components with otherwise similar efficiencies (i.e., breathing and diffusive exchange efficiencies), the one that occurs more often will be able to extract more tracer gas over time.

These three factors can be combined into the overall *barometric-pumping efficiency*  $\eta_P$  (referred to as *production efficiency* in Harp et al. (2019)), as

$$\eta_P = \eta_B \eta_D \omega. \quad (1)$$

In this study, we utilize equation 1 to discriminate factors associated with UNEs resulting in late-time seeps. Note that all the geologic factors considered here (depth of burial, air-filled porosity, matrix permeability) are included in the calculation of barometric-pumping efficiency.

**Table 1.** Site-specific UNE data.

UNE	Date	Radionuclides	Days till seep	Depth of burial [m]	Air-filled porosity [-]	Matrix permeability [m <sup>2</sup> ]
KAPPELI	7/25/84	<sup>85</sup> Kr	61	640	0.119	$1.77 \times 10^{-14}$
TIERRA	12/15/84	<sup>131m,133</sup> Xe, <sup>85</sup> Kr, <sup>37</sup> Ar	11	640	0.129	$8.07 \times 10^{-15}$
LABQUARK	9/30/86	<sup>133</sup> Xe, <sup>85</sup> Kr	25	616	0.154	$7.13 \times 10^{-15}$
BODIE	12/13/86	<sup>131m,133,133m</sup> Xe, <sup>85</sup> Kr, <sup>37</sup> Ar	2	635	0.085	$1.68 \times 10^{-14}$
BARNWELL	12/8/89	<sup>131m,133,133m</sup> Xe, <sup>85</sup> Kr	9	600	0.056	$8.17 \times 10^{-15}$
EGMONT	12/9/84	–	–	546	0.155	$1.50 \times 10^{-14}$
TOWANDA	5/2/85	–	–	665	<sup>a</sup> 0.13	$5.40 \times 10^{-15}$
SALUT	6/12/85	–	–	608	0.191	$1.58 \times 10^{-14}$
SERENA	7/25/85	–	–	597	0.103	$2.26 \times 10^{-14}$
GOLDSTONE	12/28/85	–	–	549	0.144	$1.52 \times 10^{-14}$
JEFFERSON	4/22/86	–	–	609	0.148	$1.42 \times 10^{-14}$
DARWIN	6/25/86	–	–	549	0.120	$1.47 \times 10^{-14}$
CYBAR	7/17/86	–	–	628	<sup>a</sup> 0.13	$9.27 \times 10^{-15}$
BELMONT	10/16/86	–	–	605	0.137	$7.96 \times 10^{-15}$
DELAMAR	4/18/87	–	–	544	0.157	$1.23 \times 10^{-14}$
HARDIN	4/30/87	–	–	625	0.104	$1.45 \times 10^{-14}$

<sup>a</sup>Value not available, average of values from other UNEs used.

### 3 Data

The data utilized here include geologic data and barometric pressure records for the 16 UNEs compiled by Bourret, Kwicklis, Harp, et al. (2019). We used the geologic data to assign air-filled porosity, intact-rock (matrix) permeability, and depth of burial for each UNE presented in Table 1 along with the date of the UNE, radionuclides detected, and the number of days until radionuclide gas detection after each UNE. The five UNEs where late-time seeps were observed are listed at the top of Table 1 followed by those where seeps were not observed. The air-filled porosity and matrix permeability are depth averaged properties using measured properties for the geologic layers overlying each UNE. Note that KAPPELI was the only UNE with an observed late-time seep in which an isotope of xenon was not detected (only <sup>85</sup>Kr was detected). KAPPELI also had significantly later radionuclide detection at the ground surface at 61 days after the UNE.

Bourret, Kwicklis, Harp, et al. (2019) collected the barometric records from the Weather Underground website (<https://www.wunderground.com/history>) for Mercury, NV, located just outside the southwestern entrance to the National Nuclear Security Site (NNSS). Since our analysis uses the frequencies and amplitudes of the barometric signals, and not the absolute magnitude, the barometric records were not elevation-corrected to the ground-surface elevations of the UNEs prior to analysis. In order to capture the characteristic of the barometer before and after each UNE, we included 30 days prior and 60 days after each UNE.

### 4 Results

Initially, we decomposed the barometric records for each UNE into frequency/amplitude pairs using a Fast Fourier Transform (Cooley & Tukey, 1965) algorithm. The top plot in Figure 1 presents the period/amplitude pairs, where period= $2\pi/\text{frequency}$ . The components associated with UNEs with late-time seeps are in red and those without are in blue.

We used the historical data collected by Bourret, Kwicklis, Harp, et al. (2019) to assign air-filled porosity, matrix permeability, and depth of burial for each UNE. Lacking specific details on fracture aperture and spacing for each UNE, we applied a fracture aperture of 1 mm and fracture spacing of 10 m for all UNEs. Using these decomposed period/amplitude pairs and properties, we then calculated the barometric-pumping efficiency using equation 1. We present these efficiencies in the bottom plot of Figure 1, where the barometric components associated with UNEs with late-time seeps are in red

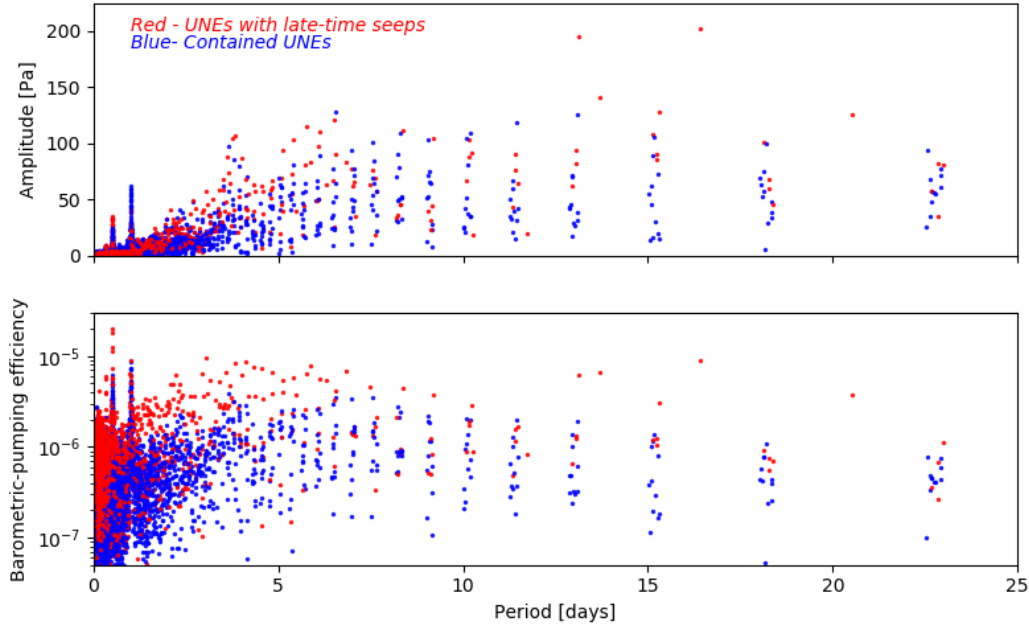


**Figure 1.** (Top) Frequency decomposition of 16 barometric signals during UNEs presented as amplitudes as a function of period. (Bottom) Barometric-pumping efficiencies of period/amplitude pairs from top plot. Red dots correspond to 5 UNEs where late-time seeps were observed. Blue dots correspond to 11 UNEs where gas seeps were not observed.

143 and those without are in blue. By inspecting the locations of red vs blue points, it is ap-  
 144 parent that, although there is significant overlap, the efficiencies for UNEs with late-time  
 145 seeps are generally higher than for those without.

146 Next, we calculated the average period and amplitude associated with the high-  
 147 est barometric-pumping efficiency components for each UNE. We accomplished this by  
 148 sorting the period/amplitude pairs in order of decreasing barometric-pumping efficiency,  
 149 smoothing the mean periods and amplitudes in this order, and then identifying the max-  
 150 imum period and amplitude of these smoothed curves. In Figure S1 of supplemental in-  
 151 formation, we present the raw and smoothed mean periods and amplitudes produced dur-  
 152 ing this analysis. This process provides a good estimate of an average period and am-  
 153 plitude associated with high-efficiency barometric components.

154 The average high-efficiency periods and amplitudes for each UNE are plotted in  
 155 the top and 2nd plot, respectively, of Figure 2. Subsequent plots in the figure contain  
 156 depth of burial, air-filled porosity, matrix permeability, and the average maximum barometric-  
 157 pumping efficiency (i.e., average of 30 highest efficiencies for each UNE) for reference.  
 158 In general, all UNEs with late-time seeps had longer high-efficiency periods and larger  
 159 high-efficiency amplitudes than those that did not. In Figure 3, we plot the average high-  
 160 efficiency periods vs average high-efficiency amplitudes to illustrate the clustering of UNEs  
 161 with late-time seeps at longer average periods and higher average amplitudes. The ex-  
 162 ception was KAPPELLI, which had different late-time seep characteristics as described  
 163 in Section 3 and discussed in Section 5.

164 In general, the UNEs with late-time seeps were deeper, although this is assumed  
 165 to be coincidental as we are not aware of a physical reason this would increase the chances  
 166 of late-time seeps. Two of the UNEs with late-time seeps (BODIE and BARNWELL)

167 had much lower air-filled porosities, which would be expected to increase the chance of  
 168 late-time seeps, while the other three had air-filled porosities similar to UNEs without  
 169 late-time seeps. The permeabilities of all UNEs varied within an order of magnitude, with  
 170 similar ranges between UNEs with late-time seeps and those without. BODIE and BARN-  
 171 WELL also had high barometric-pumping efficiencies, while KAPPELI, TIERRA, and  
 172 LABQUARK had efficiencies similar to UNEs without late-time seeps.

173 As mentioned above, the fracture aperture and spacing are not known for all the  
 174 individual UNEs; therefore, the same values were used for all UNEs. The inability to  
 175 include UNE-specific values for these factors may explain why barometric-pumping effi-  
 176 ciencies were not higher for KAPPELI, TIERRA, and LABQUARK. To investigate this  
 177 hypothesis, we analyzed the sensitivity of the barometric-pumping efficiency to UNE prop-  
 178 erties, including properties that were measured or estimated from historic data (depth  
 179 of burial, air-filled porosity, and matrix permeability). We present these sensitivities in  
 180 Figure 4, where for depth of burial, air-filled porosity, and matrix permeability, the ver-  
 181 tical gray band indicates the range of values present in the data, while for the fracture  
 182 aperture and spacing, a gray line indicates the value that was used in the analysis in lieu  
 183 of actual data. Barometric-pumping efficiency is not sensitive to depth of burial within  
 184 the range in the data, nor well beyond this range. Barometric-pumping efficiency is highly  
 185 sensitive to air-filled porosity within the range of the data, and beyond this data range.  
 186 Barometric-pumping efficiency becomes sensitive to matrix permeability at values less  
 187 than around  $10^{-15.5}$  m<sup>2</sup>, however the range of matrix permeabilities in the data is higher  
 188 than this and thus is in an insensitive region. The fracture aperture is relatively sensi-  
 189 tive even at the sub-millimeter scale, while the fracture spacing is relatively insensitive  
 190 from around 3 to 15 m, but does begin to show increased sensitivity for values less than  
 191 around 3 m.

## 192 5 Discussion

193 The results of this analysis, based on 16 UNEs from the NNSS, indicate that barometric-  
 194 pumping efficiency can facilitate the discrimination of UNEs that will result in late-time  
 195 seeps. Barometric-pumping efficiency is able to account for the character of the baro-  
 196 metric signal (frequency and amplitude), depth of burial, air-filled porosity, matrix per-  
 197 meability, fracture aperture, and fracture spacing. The differences in the period/amplitude  
 198 pairs from the UNEs with late-time seeps versus those without presented in the top plot  
 199 of Figure 1, along with the geologic data included in the analysis, result in generally higher  
 200 barometric-pumping efficiency for barometric components associated with UNEs with  
 201 late-time seeps (bottom plot of Figure 1). While there is overlap between the efficien-  
 202 cies of UNEs with and without late-time seeps, the highest barometric-pumping efficien-  
 203 cies for any given period are generally associated with a UNE with late-time seeps, and  
 204 the lowest are associated with a UNE without.

205 The barometric-pumping efficiency analysis is able to discriminate UNEs with late-  
 206 time seeps based on several factors, particularly air-filled porosity, fracture aperture, and,  
 207 for values less than around  $10^{-15.5}$  m<sup>2</sup>, matrix permeability. If values for these factors  
 208 can be well-constrained, and the characteristic of the barometric record can be obtained/forecasted  
 209 at the location shortly before and after the suspected UNE, the approach can be used  
 210 to forecast whether or not the UNE will result in late-time seeps. Barometric records  
 211 from a fairly dense network of weather stations are available globally to obtain recent  
 212 barometric pressures, fairly accurate barometric pressure forecasts out to around 10 days,  
 213 and historical records to allow extraction of barometric characteristics typical at a site.  
 214 Such information would be useful in determining the level of effort and expense that should  
 215 be expended to detect radionuclide gases at the ground surface of the site or in the at-  
 216 mosphere based on the likelihood of late-time seeps.

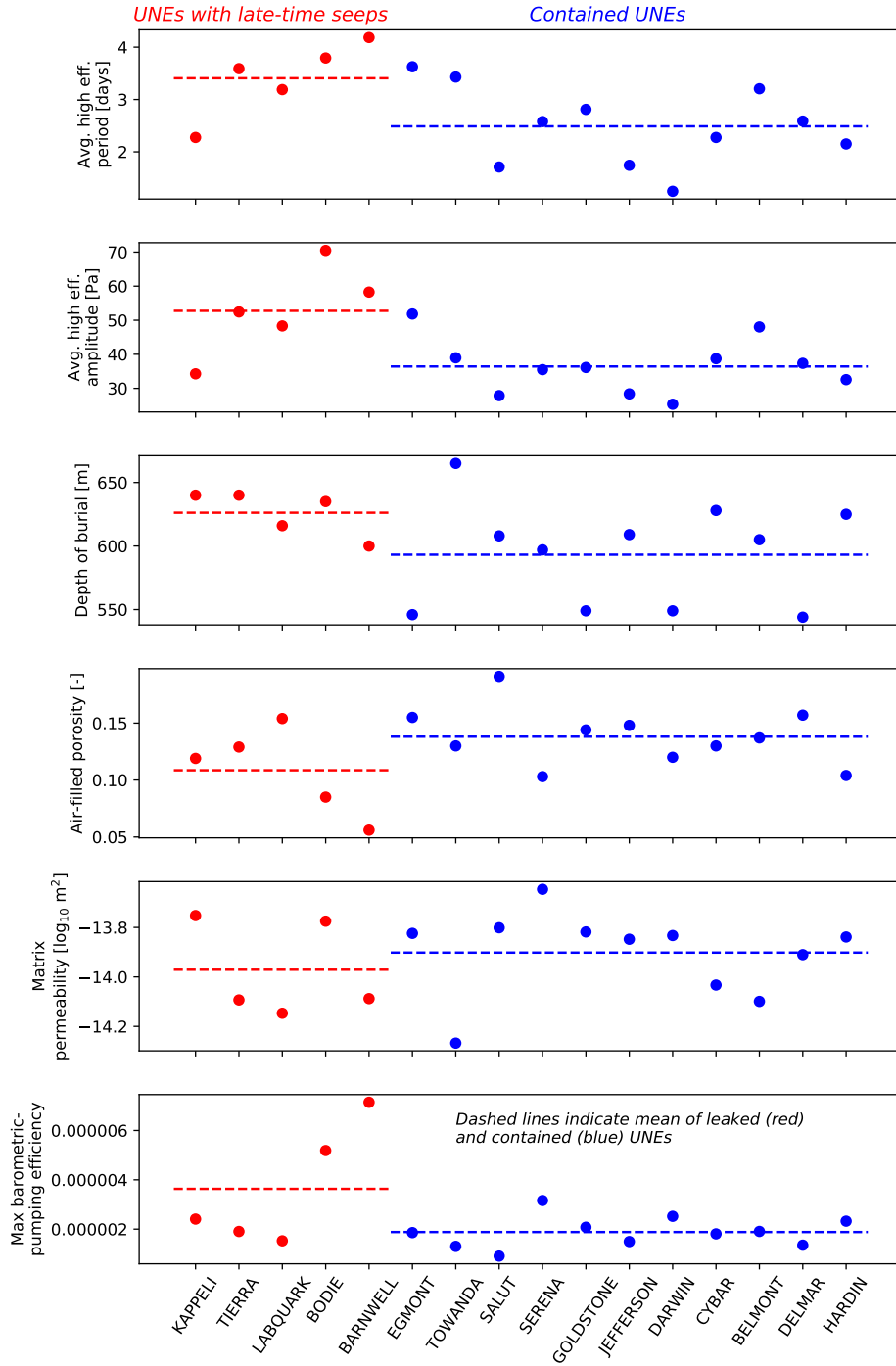


**Figure 2.** Average period (top plot) and amplitude (2nd plot) associated with high-efficiency barometric components, depth of burial (3rd plot), air-filled porosity (4th plot), matrix permeability (5th plot), and average max barometric-pumping efficiency (i.e., average of 30 highest efficiencies for each UNE) for 16 UNEs indicated on the x-axis. Red dots correspond to 5 UNEs where late-time seeps were observed. Blue dots correspond to 11 UNEs where gas seeps were not observed. Dashed lines indicate the mean value for each factor associated with UNEs with late-time seeps (red) and without (blue).

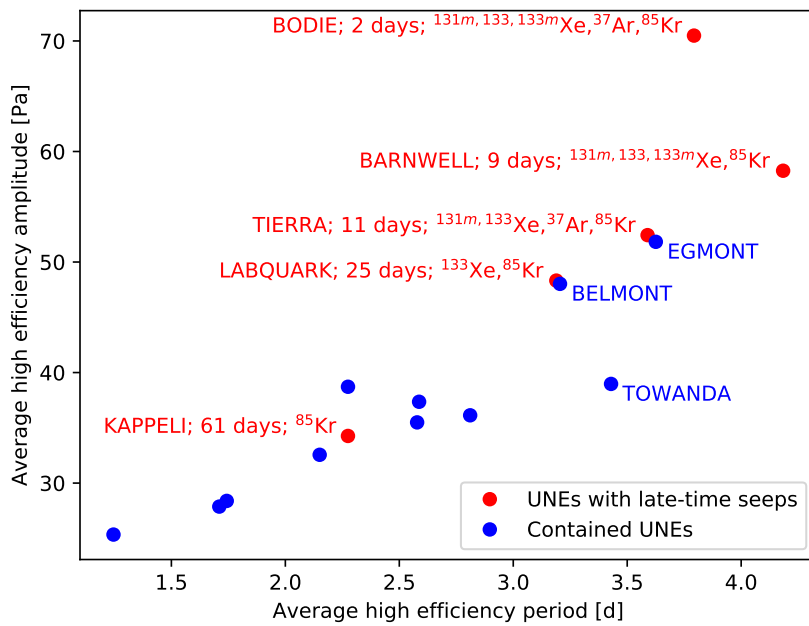


**Figure 3.** Average period versus average amplitude of high-efficiency barometric components. Red dots correspond to 5 UNEs where late-time seeps were observed. Blue dots correspond to 11 UNEs where gas seeps were not observed. The number of days till radionuclide detection after the UNE and radionuclides detected are noted.

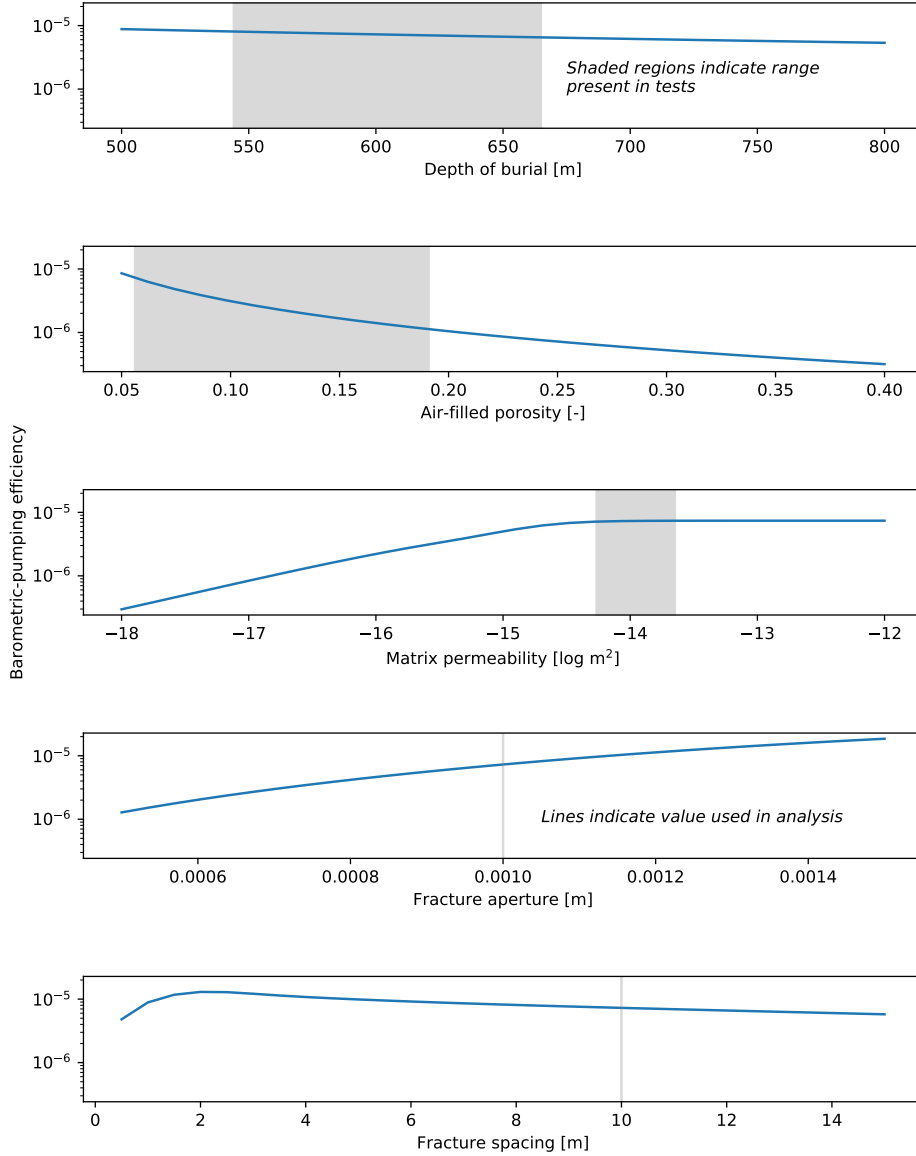


**Figure 4.** Barometric-pumping efficiency as a function of depth of burial (top plot), air-filled porosity (2nd plot), matrix permeability (3rd plot), fracture aperture (4th plot), and fracture spacing (5th plot). The range in the data from the 16 UNEs are indicated by a gray shaded region for depth of burial, air-filled porosity, and matrix permeability. The value used in the barometric-pumping efficiency analysis for fracture aperture and fracture spacing are indicated by gray lines.

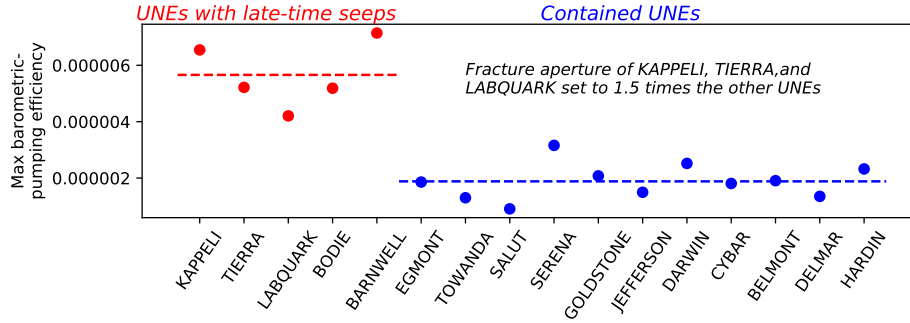


**Figure 5.** Average max barometric-pumping efficiency (i.e., average of 30 highest barometric-pumping efficiencies for each UNE) for 16 UNE's where the fracture aperture for KAPPELLI, TIERRA, and LABQUARK has been set to 1.5 mm and 1 mm for all the other UNEs.

217 The UNEs with late-time seeps have generally longer average high-efficiency peri-  
 218 ods and higher average high-efficiency amplitudes than the UNEs without (Figure 3).  
 219 The magnitudes of the average high-efficiency periods and amplitudes of UNEs without  
 220 late-time seeps decrease in general and become less distinguishable from the UNEs with-  
 221 out late-time seeps as the number of days until radionuclide detection increases (refer  
 222 to days until radionuclide detection noted in Figure 3). This suggests that the barometric-  
 223 pumping efficiency analysis is able to easily discriminate UNEs that are the most likely  
 224 to have late-time seeps (e.g., BODIE and BARNWELL), UNEs that may or may not  
 225 have late-time seeps (e.g., TIERRA (observed late-time seeps) and EGMONT (no obser-  
 226 ved late-time seeps)), and UNEs that are likely to remain contained. Note that KAP-  
 227 PELLI was unique in the set of UNEs with late-time seeps in that it took much longer  
 228 to seep (more than twice as long as any other UNE) and no xenon isotopes were detected,  
 229 only  $^{85}\text{Kr}$ . The UNEs without observed late-time seeps which had higher high-efficiency  
 230 amplitudes and longer high-efficiency periods labeled in Figure 3 (EGMONT, TOWANDA,  
 231 and BELMONT) do not have distinguishable geologic properties in common compared  
 232 to the other UNEs without observed late-time seeps or that can distinguish them from  
 233 UNEs with late-time seeps with similar high-efficiency periods and amplitudes (TIERRA  
 234 and LABQUARK) (refer to Figure 2).

235 If knowledge was available regarding the fracture aperture, and to a lesser extent,  
 236 the fracture spacing, further separation between the efficiencies of UNEs with late-time  
 237 seeps vs those without may occur. For example, we demonstrate in Figure 5 that by sim-  
 238 ply increasing the fracture aperture associated with KAPPELLI, TIERRA, and LABQUARK  
 239 by half a millimeter (from 1 mm to 1.5 mm), their efficiencies become comparable to BODIE  
 240 and BARNWELL and distinct from the UNEs without observed late-time seeps. Of course,  
 241 there is no basis for this modification, but it does indicate that a small change in frac-  
 242 ture properties can have a large effect on barometric-pumping efficiency and that the avail-  
 243 ability of this information can greatly constrain the analysis.

244 Barometric-pumping efficiency does not consider the UNE yield. The unclassified  
 245 yield of the 16 UNEs considered here is 20-150 kt; therefore, differences in yield between  
 246 these bounds may also explain why some had late-time seeps and others did not. Barometric-  
 247 pumping efficiency also does not consider the pressurization and thermal effects on gas  
 248 transport that would be associated with a UNE, which will be a function of yield. While  
 249 these effects may help discriminate UNEs with late-time seeps, Bourret, Kwicklis, Miller,  
 250 and Stauffer (2019) found that considering barometrically-induced gas seepage alone al-

251 lowed numerical simulations of BARNWELL to produce consistent results with late-time  
 252 seep measurements.

## 253 6 Conclusions

- 254 • UNEs with late-time seeps generally have higher barometric-pumping efficiencies  
 255 than those without.
- 256 • UNEs with late-time seeps generally have higher high-efficiency amplitudes and  
 257 longer high-efficiency periods than those without.
- 258 • The most sensitive geologic factors to aid in discriminating UNEs that are likely  
 259 to have late-time seeps are air-filled porosity, fracture aperture, and matrix per-  
 260 meability ( $< 5 \times 10^{-15} \text{ m}^2$ )
- 261 • For the 5 UNEs with late-time seeps evaluated here, the time to detect a late-time  
 262 seep decreases as the high-efficiency amplitudes and period lengths increase.
- 263 • UNEs with the shortest time to radionuclide gas detection had the highest high-  
 264 efficiency amplitudes and longest high-efficiency periods, indicating that they are  
 265 likely easier to discriminate.

## 266 Acknowledgments

267 This research is supported by National Nuclear Security Administration Office of De-  
 268 fense Nuclear Nonproliferation Research and Development and the Defense Threat Re-  
 269 duction Agency. Los Alamos National Laboratory completed this work under the aus-  
 270 pices of the U.S. Department of Energy under contract DE-AC52-06NA24596 and 89233218CNA000001.  
 271 The authors acknowledge the use of barometric pressure data from Weather Underground  
 272 ([www.wunderground.com](http://www.wunderground.com)).

## 273 References

- 274 Auer, L. H., Rosenberg, N. D., Birdsell, K. H., & Whitney, E. M. (1996, November).  
 275 The effects of barometric pumping on contaminant transport. *Journal of Con-*  
 276 *taminant Hydrology*, *24*(2), 145–166. Retrieved from [http://dx.doi.org/10](http://dx.doi.org/10.1016/S0169-7722(96)00010-1)  
 277 [.1016/S0169-7722\(96\)00010-1](http://dx.doi.org/10.1016/S0169-7722(96)00010-1) doi: 10.1016/S0169-7722(96)00010-1
- 278 Bourret, S. M., Kwicklis, E. M., Harp, D. R., Ortiz, J. P., & Stauffer, P. H. (2019).  
 279 Beyond BARNWELL: Applying lessons learned from the BARNWELL site  
 280 to other historic underground nuclear tests at Pahute Mesa to understand  
 281 radioactive gas-seepage observations. *Hydrological Processes*. (In review)
- 282 Bourret, S. M., Kwicklis, E. M., Miller, T. A., & Stauffer, P. H. (2019). Evaluating  
 283 the importance of barometric pumping for subsurface gas transport near an  
 284 underground nuclear test site. *Vadose Zone Journal*, *18*(1).
- 285 Cooley, J. W., & Tukey, J. W. (1965). An algorithm for the machine calculation of  
 286 complex fourier series. *Mathematics of computation*, *19*(90), 297–301.
- 287 Harp, D. R., Ortiz, J. P., Pandey, S., Karra, S., Anderson, D., Bradley, C., ...  
 288 Stauffer, P. H. (2018). Immobile pore-water storage enhancement and re-  
 289 tardation of gas transport in fractured rock. *Transport in Porous Media*,  
 290 *124*(2), 369–394.
- 291 Harp, D. R., Ortiz, J. P., & Stauffer, P. H. (2019). Identification of dominant gas  
 292 transport frequencies during barometric pumping of fractured rock. *Scientific*  
 293 *reports*, *9*(1), 9537.
- 294 Jordan, A. B., Stauffer, P. H., Zyzolowski, G. A., Person, M. A., MacCarthy, J. K., &  
 295 Anderson, D. N. (2014). Uncertainty in prediction of radionuclide gas migra-  
 296 tion from underground nuclear explosions. *Vadose Zone Journal*, *13*(10).
- 297 Kalinowski, M., Axelsson, A., Bean, M., Blanchard, X., Bowyer, T., Brachet,  
 298 G., ... Kurt Ungar, R. (2010, May 1). Discrimination of Nuclear Ex-

- 299 plusions against Civilian Sources Based on Atmospheric Xenon Isotopic  
300 Activity Ratios. *Pure and Applied Geophysics*, 167(4-5), 517–539. Re-  
301 trieved from <http://dx.doi.org/10.1007/s00024-009-0032-1> doi:  
302 10.1007/s00024-009-0032-1
- 303 Neeper, D. A. (2003, February). Harmonic analysis of flow in open boreholes due to  
304 barometric pressure cycles. *Journal of Contaminant Hydrology*, 60(3-4), 135–  
305 162. Retrieved from [http://dx.doi.org/10.1016/s0169-7722\(02\)00086-4](http://dx.doi.org/10.1016/s0169-7722(02)00086-4)  
306 doi: 10.1016/s0169-7722(02)00086-4
- 307 Neeper, D. A., & Stauffer, P. H. (2012). Transport by oscillatory flow in soils with  
308 rate-limited mass transfer: 1. theory. *Vadose Zone Journal*, 11(2).
- 309 Nilson, R. H., Peterson, E. W., Lie, K. H., Burkhard, N. R., & Hearst, J. R. (1991,  
310 December 10). Atmospheric pumping: A mechanism causing vertical trans-  
311 port of contaminated gases through fractured permeable media. *J. Geophys.*  
312 *Res.*, 96(B13), 21933–21948. Retrieved from [http://dx.doi.org/10.1029/  
313 91jb01836](http://dx.doi.org/10.1029/91jb01836) doi: 10.1029/91jb01836
- 314 Sun, Y., & Carrigan, C. (2014, July 7). Modeling Noble Gas Transport and De-  
315 tection for The Comprehensive Nuclear-Test-Ban Treaty. *Pure and Applied*  
316 *Geophysics*, 171(3-5), 735–750. Retrieved from [http://dx.doi.org/10.1007/  
317 s00024-012-0514-4](http://dx.doi.org/10.1007/s00024-012-0514-4) doi: 10.1007/s00024-012-0514-4
- 318 Sun, Y., & Carrigan, C. R. (2016). Thermally driven advection for radioxenon  
319 transport from an underground nuclear explosion. *Geophysical Research Let-*  
320 *ters*, 43(9), 4418–4425.
- 321 United States Congress. (1989). *The containment of underground nuclear explosions.*  
322 Congress of the US, Office of Technology Assessment.